Decision Fusion for Carbon Dioxide Release Detection from Pressure Relief Devices

Gianluca Tabella*†, Yuri Di Martino, Domenico Ciuonzo‡, Nicola Paltrinieri§, Xiaodong Wang†, and Pierluigi Salvo Rossi*¶

*Dept. Electronic Systems, Norwegian University of Science and Technology, Trondheim, Norway
†Dept. Electrical Engineering, Columbia University, New York, NY, USA
‡Dept. Electrical Engineering and Information Technologies (DIETI), University of Naples "Federico II", Naples, Italy
§Dept. Mechanical and Industrial Engineering, Norwegian University of Science and Technology, Trondheim, Norway
¶Dept. Gas Technology, SINTEF Energy Research, Norway
Email: gianluca.tabella@ntnu.no; yuri.di.martino@gmail.com; domenico.ciuonzo@unina.it; nicola.paltrinieri@ntnu.no; wangx@ee.columbia.edu; salvorossi@ieee.org

2022 IEEE 12th Sensor Array and Multichannel Signal Processing Workshop (SAM) | 978-1-6654-0633-8/22/$31.00 ©2022 IEEE | DOI: 10.1109/SAM53842.2022.9827715

***Abstract*—This work investigates the distributed detection of carbon dioxide (CO_2) release from storage tanks caused by the opening of pressure relief devices via inexpensive sensor devices in an industrial context. A realistic model of the dispersion is put forward in this paper. Both full-precision and rate-limited setups for sensors are considered, and fusion rules capitalizing the dispersion model are derived. Simulations analyze the performance trends with relevant system parameters.**

***Index Terms*—Carbon Dioxide, Decision Fusion, Distributed Detection, Industry 4.0, Internet of Things, Wireless Sensor Networks.**

I. Introduction

The last decades have seen the growth of Wireless Sensor Networks (WSNs) due to their collective, cost-effective, and successful use in monitoring applications. In particular, the task of harmful-event discovery has received large attention in the last years. Relevant scenarios include counter-terrorism and safety in Industry 4.0. The associated inference problems are related to source localization and "early" detection [1]. In this context, most of the works only assume a Gaussian plume point source model based on diffusion/advection processes, e.g. with application to dispersion of biochemical moving sources [2], [3], localization of atmospheric pollutants [4] and release of light gases [5]. On the contrary, *carbon dioxide* (CO_2) is a (heavy) gas whose density, at atmospheric temperature and pressure, is about 1.5 larger than the air density and is present in atmosphere at average concentration ≈ 400 ppm, as of today. Nowadays, CO_2 finds several applications at domestic and industrial levels [6], [7]. Unluckily, when CO_2 is stored, it is possible that accidental releases occur with the main danger of asphyxiation. We remark that CO_2 *does not adhere* to neutral or positively-buoyant dispersion behavior.

For bulk storage, CO_2 is typically stored as liquid in insulated tanks[1] (see Fig. 1), usually equipped with systems to limit the internal pressure, namely *pressure relief devices* (PRDs). These can be safety valves, rupture disks, or their combinations. PRDs are designed in accordance to international or national standards to protect the vessel when the internal pressure exceeds the *maximum allowable working pressure* (MAWP). The causes of overpressure may be several, ranging from process upsets to external fires. In any of these cases, the PRD must release the flow rate necessary to avoid dangerous pressure build-up inside the tank. In such cases, however, the consequences of PRD activation can still be harmful to human life and accurate detection of these critical events should be performed leveraging WSNs.

To this end, Industrial IoT, with inexpensive sensors and the possibility of leveraging collective analytics to obtain improved performance, represents an enabler for this task. However, due to their stringent bandwidth and energy constraints toward close-to-perpetual lifetime of IoT devices, sensors are usually constrained to send extremely-compressed versions of their measurements to a Fusion Center (FC). For this reason, the localization of the same diffusive sources via WSNs has shifted toward the use of binary sensors [9], [10].

Accordingly, the *contributions* of this work are as follows. We model the release of CO_2 from PRDs via a more appropriate *Britter & McQuaid* (B&M) model and include unavoidable fluctuations in the concentration. The sensors measure the concentration and report only one bit to the FC, targeting an industrial IoT setup with small-battery (low-energy) sensors. Since the activated PRD is unknown, the FC is in charge of performing decision fusion by tackling a composite hypothesis testing. For the mentioned reason, a generalized likelihood ratio (GLR)-based fusion rule is devised and compared with a GLR counterpart based on full-precision measurements and the counting rule. Simulation results highlight the need for fusion rules weighting sensors' decisions according to a practical CO_2 release model.

The rest of the paper is organized as follows: Sec. II describes the considered system model, whereas Secs. III and IV introduce the proposed decision fusion approach for CO_2 release detection. Our approach is then numerically validated on a real case study in Sec. V. Sec. VI ends the paper with

This research is a part of BRU21 – NTNU Research and Innovation Program on Digital and Automation Solutions for the Oil and Gas Industry (www.ntnu.edu/bru21).

[1]Storage temperature is below ambient temperature, typically $\in [-30, -20]$°C with corresponding pressures of $\in [14.3, 19.7]$ bar [7], [8].

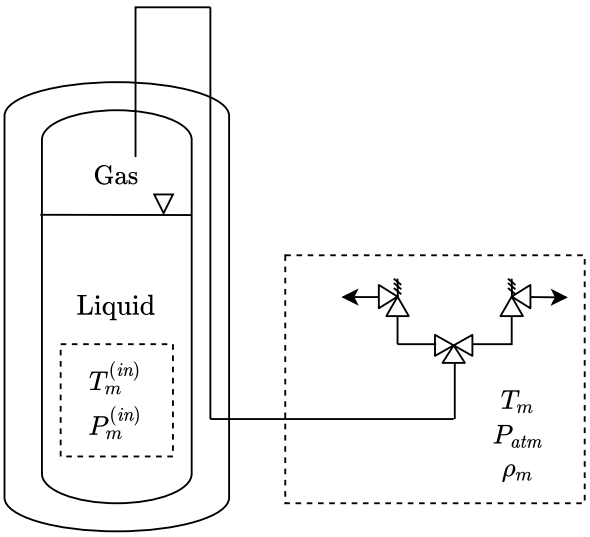

Fig. 1: Scheme of the tank and its PRD with the corresponding thermodynamic conditions.

some pointers to future directions of research.[2]

II. System Model

WSN model: The examined industrial facility consists of M vessels containing liquefied CO_2 and their respective PRDs. The plant is monitored by K concentration sensors individually assessing the absence ($\mathcal{H}_0$) or presence ($\mathcal{H}_1$) of a gas dispersion by measuring the local gas concentration y_k and reporting their local decision $d_k = i$, if $\mathcal{H}_i$ is declared as reported in Fig. 2. Binary decisions are spectrally efficient, as only 1-bit communication is required on the communication channel between the sensor and the FC, as well as being energy-efficient when OOK is employed [11], [12]. The vector of local decisions $\boldsymbol{d} = \begin{bmatrix} d_1 & \cdots & d_K \end{bmatrix}^T$ is acquired by the FC that processes it and takes a global decision $\widehat{\mathcal{H}} \in \{\mathcal{H}_0, \mathcal{H}_1\}$. As a comparative tool, the WSN is also examined in the case in which the FC acquires full-precision measurements $\boldsymbol{y} = \begin{bmatrix} y_1 & \cdots & y_K \end{bmatrix}^T$ from the sensors.

Dispersion model: The heavy gas dispersion model used herein is based on the well-known B&M for continuous release [13]–[18]. The output of the dispersion model allows the evaluation of the *average molar fraction concentration* at the kth sensor when the mth PRD is open, denoted with $c_{k,m}$. Inside the tank corresponding to the mth valve there exists a CO_2 liquid-vapor equilibrium at a certain pressure $P_m^{(in)} > P_{atm}$ and the corresponding saturation temperature $T_m^{(in)} = T_{sat}\left(P_m^{(in)}\right)$, where *atm* stands for *atmospheric* and

[2]*Notation* – Bold letters denote vectors; $(\cdot)^T$ denotes transpose; $\hat{a}$ denote an estimate of the random variable a; $\Pr(\cdot)$ and $p(\cdot)$ denote probability mass functions (pmfs) and probability density functions (pdfs), while $\Pr(\cdot|\cdot)$ and $p(\cdot|\cdot)$ their corresponding conditional counterparts; $F_a(\cdot)$ is the cumulative distribution function (cdf) of the random variable a and $F_{a|b}(\cdot)$ is its conditional counterpart given the random variable b; Gamma (α, β) denotes a Gamma distribution with shape α and rate β; $\Gamma(\cdot)$ is the Gamma function; the symbol $\sim$ (resp. $\overset{\text{approx.}}{\sim}$) means "distributed as" (resp. "approximately distributed as"); finally $\mathcal{O}(\cdot)$ denotes the big O notation.

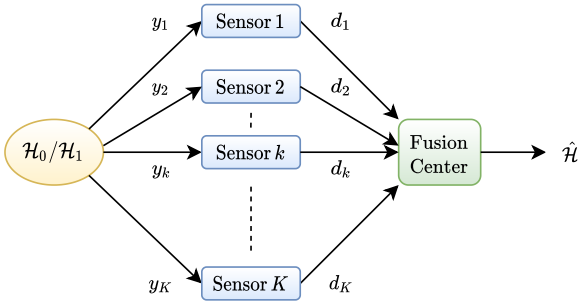

Fig. 2: Wireless Sensor Network Architecture.

sat for *saturation*. When $P_m^{(in)}$ reaches the PRD set pressure, the device opens, releasing the gas phase in atmosphere. At this point a *Joule-Thompson process* occurs with a consequent (isenthalpic) expansion and cooling of the gas[3]. At release condition, the gas will be at a temperature T_m, pressure P_{atm}, and a certain density ρ_m. T_m and ρ_m can be obtained through an appropriate equation of state (EOS) using $T_m^{(in)}$ and $P_m^{(in)}$ as inputs (see Fig. 1). As well as the previous thermodynamic properties, the B&M model requires the following parameters for its use: the atmospheric temperature (T_{atm}), the density of air at T_{atm} (ρ_{air}), the volumetric flow rate from the mth PRD ($\dot{V}_m$), the wind speed at a height of 10 m (u) and its direction (φ)[4], the mth PRD's diameter (D_m), and the concentration at release condition from the mth PRD (c_m).[5]

Signal Model: When a PRD opens, the released gas affects its value of concentration in the surrounding environment. The following equations describe the concentration (y_k) measured by kth sensor in terms in the case of normal operations ($\mathcal{H}_0$), and in the case of an open PRD ($\mathcal{H}_1$):

$$\begin{cases} \mathcal{H}_0: & y_k = w_k \\ \mathcal{H}_1: & y_k = c_{k,m} \cdot \xi_k + w_k \end{cases}, \tag{2}$$

where $w_k \sim \text{Gamma}\left(\frac{b^2}{\nu^2}, \frac{b}{\nu^2}\right)$ is the concentration present in atmosphere in normal conditions with b as its mean value and ν as its standard deviation. $c_{k,m}$ is the mean value of concentration contribution where the kth sensor is located due to the opening of the mth PRD. Finally, $\xi_k \sim \text{Gamma}\left(\omega^{-2}, \omega^{-2}\right)$ is the fluctuation around the value of $c_{k,m}$, where ω is the relative mean fluctuation [19]. Due to the spatial separation of the sensors, ξ_k's and w_k's are both assumed statistically independent. Treating $p(y_k|\mathcal{H}_1; m)$ is not trivial, being the sum of two Gamma random variables: hence, we approximate it with

[3]We neglect possible formation of liquid or solid during this transformation.

[4]Wind blowing from north: 0° (360°), east: 90°, south: 180°, west: 270°.

[5]The B&M model is meant for continuous release of heavy gases meeting the following criterion:

$$\frac{g^2 \left(\rho_m - \rho_{air}\right)^2 \dot{V}_m^{0.5}}{u^{2.5} \rho_{air}^2} \geq 3.375 \times 10^{-3}, \tag{1}$$

where g is the gravitational acceleration. Limitations that can affect the accuracy of the result are: the release and the calculated concentrations are assumed to be at ground level; the concentration in the plume's cross-sectional area is assumed uniform; the jet due to a high-velocity release is not modeled; obstacles are not modeled; low distances from the source cause higher errors.

a single Gamma random variable via *moment matching* [20]. The approximated signal's distribution then becomes:

$$\begin{cases} y_k|\mathcal{H}_0 \sim \text{Gamma}\left(\alpha^{(0)}, \beta^{(0)}\right) \\ y_k|\mathcal{H}_1; m \overset{\text{approx.}}{\sim} \text{Gamma}\left(\alpha_{k,m}^{(1)}, \beta_{k,m}^{(1)}\right) \end{cases}, \tag{3}$$

where $\alpha^{(0)} \triangleq \frac{b^2}{\nu^2}$, $\beta^{(0)} \triangleq \frac{b}{\nu^2}$, $\alpha_{k,m}^{(1)} \triangleq \frac{(c_{k,m}+b)^2}{\omega^2 c_{k,m}^2+\nu^2}$, and $\beta_{k,m}^{(1)} \triangleq \frac{c_{k,m}+b}{\omega^2 c_{k,m}^2+\nu^2}$.

III. Local Detection

As a consequence of Eq. (3), we can write the likelihoods of a sensor measurement as:

$$p(y_k|\mathcal{H}_i) = \frac{{\beta^{(i)}}^{\alpha^{(i)}}}{\Gamma\left(\alpha^{(i)}\right)} y_k^{\alpha^{(i)}-1} e^{-\beta^{(i)} y_k}, \qquad i \in \{0,1\}. \tag{4}$$

Note that $p(y_k|\mathcal{H}_i)$, $\alpha^{(1)}$, and $\beta^{(1)}$ are always referred to as $p(y_k|\mathcal{H}_1; m)$, $\alpha_{k,m}^{(1)}$, and $\beta_{k,m}^{(1)}$, respectively. One should also keep in mind that Eq. (4), for $i = 1$, is an approximated pdf, and that such approximation will propagate throughout many of the equations in the rest of the work. At kth sensor, the log-likelihood ratio test on y_k is *uniformly most powerful* (UMP) in local sense leading to the following test:

$$\ln y_k - \left[\left(\beta_{k,m}^{(1)} - \beta^{(0)}\right) \Big/ \left(\alpha_{k,m}^{(1)} - \alpha^{(0)}\right)\right] y_k \underset{d_k=0}{\overset{d_k=1}{\gtrless}} \gamma. \tag{5}$$

Eq. (5) shows that the detector needs the values of $\alpha_{k,m}^{(1)}$ and $\beta_{k,m}^{(1)}$ to implement a UMP test. Unluckily, these values are not available for the sensors as they depend on the current wind speed and direction (which change over time), as well as the unknown parameter m. This suggests considering a (simpler) concentration level test having computational complexity $\mathcal{O}(1)$ in lieu of Eq. (5), namely:

$$y_k \underset{d_k=0}{\overset{d_k=1}{\gtrless}} \gamma. \tag{6}$$

The performance of this test is obtained thanks to the approximation carried out in Eq. (3):

$$P_{D,k}(m) \triangleq \Pr(y_k \geq \gamma|\mathcal{H}_1; m) = 1 - F_{y_k|\mathcal{H}_1;m}(\gamma), \tag{7}$$

$$P_F \triangleq \Pr(y_k \geq \gamma|\mathcal{H}_0) = 1 - F_{y_k|\mathcal{H}_0}(\gamma). \tag{8}$$

The Neyman-Pearson approach is here employed to design the threshold γ by fixing the desired value of P_F.

IV. Fusion Center

Centralized GLRT: In the case where the sensors transmit the raw measurements to the FC we exploit conditional independence $p(\boldsymbol{y}|\mathcal{H}_1; m) = \prod_{k=1}^{K} p(y_k|\mathcal{H}_1; m)$ and Eq. (4) to obtain likelihood under $\mathcal{H}_1$. Similarly, one can obtain $p(\boldsymbol{y}|\mathcal{H}_0)$ replacing $p(y_k|\mathcal{H}_1; m)$ with $p(y_k|\mathcal{H}_0)$. In such a scenario, a centralized GLRT (C-GLRT) fusion rule can be employed:

$$\begin{aligned} \Lambda_{\text{C-GLRT}} &= \ln\left[\max_{m=1,\dots,M} \frac{p(\boldsymbol{y}|\mathcal{H}_1; m)}{p(\boldsymbol{y}|\mathcal{H}_0)}\right] \\ &= \sum_{k=1}^{K} \ln\left[\frac{p(y_k|\mathcal{H}_1; \widehat{m}_{\text{C}})}{p(y_k|\mathcal{H}_0)}\right] \underset{\widehat{\mathcal{H}}=\mathcal{H}_0}{\overset{\widehat{\mathcal{H}}=\mathcal{H}_1}{\gtrless}} \overline{\gamma}, \end{aligned} \tag{9}$$

where $\widehat{m}_{\text{C}}$ is the Maximum Likelihood Estimate (MLE) of m when $\mathcal{H}_1$ holds, namely $\widehat{m}_{\text{C}} = \underset{m=1,\dots,M}{\arg\max} \sum_{k=1}^{K} \ln p(y_k|\mathcal{H}_1; m)$. This fusion rule has computational complexity $\mathcal{O}(KM)$.

Distributed GLRT: When the sensors transmit binary decisions, the corresponding likelihood is $\Pr(\boldsymbol{d}|\mathcal{H}_1; m) = \prod_{k=1}^{K} \left[P_{D,k}(m)^{d_k}(1 - P_{D,k}(m))^{1-d_k}\right]$. Similarly, one obtains $\Pr(\boldsymbol{d}|\mathcal{H}_0)$ replacing $P_{D,k}(m)$ with P_F. In this case, the FC can perform a Generalized version of the well-known Chair-Varshney Rule, or Distributed GLRT (D-GLRT):

$$\begin{aligned} \Lambda_{\text{D-GLRT}} &= \ln\left[\max_{m=1,\dots,M} \frac{\Pr(\boldsymbol{d}|\mathcal{H}_1; m)}{\Pr(\boldsymbol{d}|\mathcal{H}_0)}\right] \\ &= \sum_{k=1}^{K} \left[d_k \ln \frac{P_{D,k}(\widehat{m}_{\text{D}})}{P_F} \right. \\ &\qquad \left. + (1 - d_k) \ln \frac{1 - P_{D,k}(\widehat{m}_{\text{D}})}{1 - P_F}\right] \underset{\widehat{\mathcal{H}}=\mathcal{H}_0}{\overset{\widehat{\mathcal{H}}=\mathcal{H}_1}{\gtrless}} \overline{\gamma}, \end{aligned} \tag{10}$$

where $\widehat{m}_{\text{D}}$ is the MLE of m when $\mathcal{H}_1$ holds, namely $\widehat{m}_{\text{D}} = \underset{m=1,\dots,M}{\arg\max} \sum_{k=1}^{K} \ln \Pr(d_k|\mathcal{H}_1; m)$. As before, the computational complexity is $\mathcal{O}(KM)$.

Counting Rule (CR): The well-known CR is among the simplest fusion rules, where the number of sensors detecting a dispersion is compared to a threshold:

$$\Lambda_{\text{CR}} = \sum_{k=1}^{K} d_k \underset{\widehat{\mathcal{H}}=\mathcal{H}_0}{\overset{\widehat{\mathcal{H}}=\mathcal{H}_1}{\gtrless}} \overline{\gamma}. \tag{11}$$

Unlike GLR fusion rules, the CR does not require the likelihood of $\boldsymbol{d}$ and has the lower computational complexity $\mathcal{O}(K)$.

V. Simulation Results

The results are obtained simulating a plant containing $K = 8$ sensors and $M = 2$ PRDs assumed to be identical to facilitate the discussion of the results. The geometrical configuration can be seen in Fig. 3. Because of the symmetry of the monitored area, the simulations always consider the upper PRD ($m = 1$) to be open. Simulation parameters are collected in Tab. I. From Fig. 4, it is immediately noticeable the superiority of the C-GLRT since directly transmitting $\boldsymbol{y}$ rather than $\boldsymbol{d}$ to the FC shows its benefits. However, such a network will likely show higher operating costs than a distributed network, especially in case of frequent measurements and transmissions to the FC. When considering one-bit quantization, we notice how in general the D-GLRT rule gives better performance than the CR. This highlights how a model-aware design of the FC has its benefits compared to a heuristic design (remember that the CR can be implemented with no knowledge of the signal model). It is important to remember that while the CR allows only K thresholds, the D-GLRT allows $\left(2^K - 1\right) M$ thresholds making it more versatile. It is interesting to notice the high dependency of the ROC curve with respect to the wind characteristics. Fig. 4a shows the best performances among the tested directions. This is because in

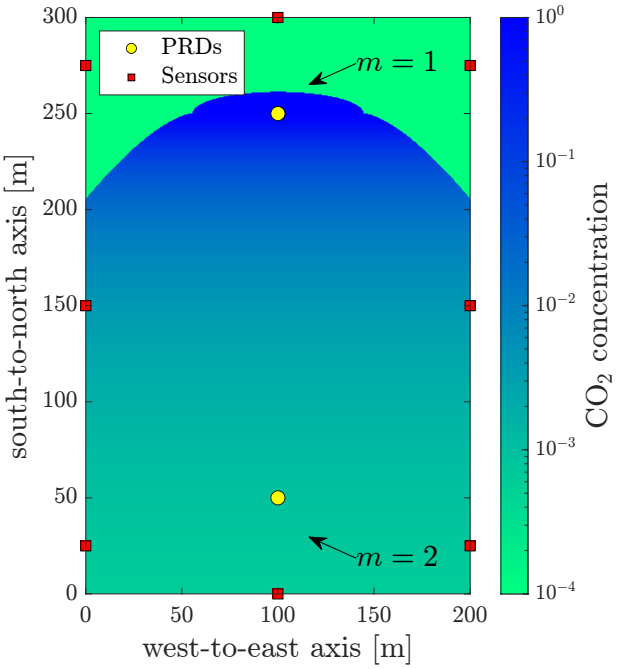

Fig. 3: (Mean) concentration map with dispersion from the upper PRD ($m = 1$) and wind blowing from north ($\varphi = 0°$).

TABLE I: Parameters used for the simulation

Parameter	Value	Note
c_m	1	$\forall m$, pure CO_2
$T_m^{(in)}$	253 K	$\forall m$, [8]
T_m	219 K	$\forall m$, *Soave-Redlich–Kwong* EOS [21]
T_{atm}	293 K	–
$P_m^{(in)}$	19.8 bar	$\forall m$
P_{atm}	1.0 bar	–
ρ_m	2.48 kg/m^3	$\forall m$, *Soave-Redlich–Kwong* EOS [21]
ρ_{air}	1.20 kg/m^3	[22]
u	1 m/s	–
$\dot{V}_m$	0.5312 m^3/s	$\forall m$
D_m	17.98 mm	$\forall m$
b	400 ppm	–
ν	200 ppm	–
ω	1	–
γ	985 ppm	from Eq. (8) with $P_F = 0.05$

such case the CO_2 plume reaches most of the sensors (see Fig. 3). In the scenarios in Figs. 4b and 4c, instead, fewer sensors notice any effect due to $\mathcal{H}_1$ being true. In these cases it is even more vital to have a FC that integrates the model. In such case, in fact, the D-GLRT weighs the different d_k's integrating the knowledge of the different c_{km}'s and the signal distribution to compute the values of the $P_{D,K}(m)$'s.

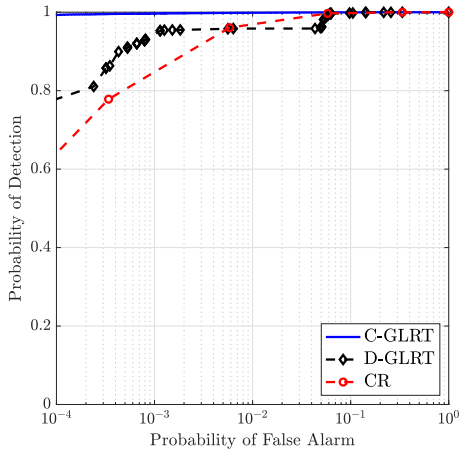

(a) Wind blowing from north ($\varphi = 0°$).

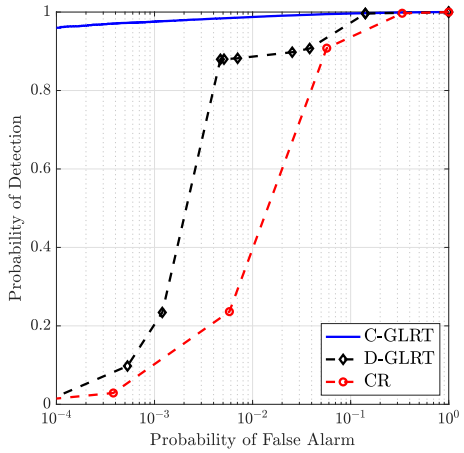

(b) Wind blowing from west ($\varphi = 270°$).

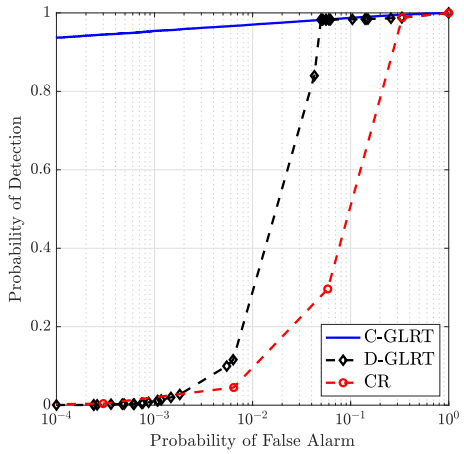

(c) Wind blowing from south ($\varphi = 180°$).

Fig. 4: ROC curves at different wind directions.

VI. Conclusions and Future Directions

In this work, we addressed the distributed detection (via a WSN) of CO_2 release from storage tanks caused by the opening of PRDs. The sensors individually monitor the facility and transmit their decisions to a FC based on individual on a concentration level test. Herein, a spatial aggregation is performed, based on GLRT and a global decision is performed. Results have highlighted the benefit in terms of ROC with respect to the well-known CR that does not include the knowledge of the dispersion model in its design. Future directions will include: (a) source localization, (b) sequential algorithms, and (c) more complex dispersion models.

REFERENCES

[1] M. Ortner and A. Nehorai, "A sequential detector for biochemical release in realistic environments," *IEEE Transactions on Signal Processing*, vol. 55, no. 8, pp. 4173–4182, 2007.

[2] T. Zhao and A. Nehorai, "Detecting and estimating biochemical dispersion of a moving source in a semi-infinite medium," *IEEE Transactions on Signal Processing*, vol. 54, no. 6, pp. 2213–2225, 2006.

[3] S. Aldalahmeh, M. Ghogho, and A. Swami, "Fast distributed detection, localization, and estimation of a diffusive target in wireless sensor networks," in *7th International Symposium on Wireless Communication Systems*. IEEE, 2010, pp. 882–886.

[4] B. Ristic, A. Gunatilaka, and R. Gailis, "Achievable accuracy in gaussian plume parameter estimation using a network of binary sensors," *Information Fusion*, vol. 25, pp. 42–48, 2015.

[5] S. Vijayakumaran, Y. Levinbook, and T. F. Wong, "Maximum likelihood localization of a diffusive point source using binary observations," *IEEE Transactions on Signal Processing*, vol. 55, no. 2, pp. 665–676, 2007.

[6] Y. Di Martino, S. E. Duque, G. Reniers, and V. Cozzani, "Making the chemical and process industries more sustainable: Innovative decision-making framework to incorporate technological and non-technological inherently safer design (ISD) opportunities," *Journal of Cleaner Production*, vol. 296, p. 126421, 2021.

[7] P. Harper, *Assessment of the major hazard potential of carbon dioxide (CO_2)*. UK: Health and Safety Executive, 2011.

[8] NIST, "Thermophysical Properties of Carbon dioxide," 2022.

[9] B. Ristic, A. Gunatilaka, and R. Gailis, "Localisation of a source of hazardous substance dispersion using binary measurements," *Atmospheric Environment*, vol. 142, pp. 114–119, 2016.

[10] D. D. Selvaratnam, I. Shames, D. V. Dimarogonas, J. H. Manton, and B. Ristic, "Co-operative estimation for source localisation using binary sensors," in *56th IEEE Annual Conference on Decision and Control (CDC)*, 2017, pp. 1572–1577.

[11] A. Shoari, G. Mateos, and A. Seyedi, "Analysis of target localization with ideal binary detectors via likelihood function smoothing," *IEEE Signal Processing Letters*, vol. 23, no. 5, pp. 737–741, 2016.

[12] G. Tabella, N. Paltrinieri, V. Cozzani, and P. Salvo Rossi, "Wireless sensor networks for detection and localization of subsea oil leakages," *IEEE Sensors Journal*, vol. 21, no. 9, pp. 10 890–10 904, 2021.

[13] R. E. Britter and J. McQuaid, *Workbook on the dispersion of dense gases*. UK: Health and Safety Executive, 1988.

[14] S. Hanna, "Britter and McQuaid (B&M) 1988 workbook nomograms for dense gas modeling applied to the Jack Rabbit II chlorine release trials," *Atmospheric Environment*, vol. 232, p. 117539, 2020.

[15] TNO, *Yellow Book – Methods for the calculation of physical effects*. The Hague, The Netherlands: The Committee for the Prevention of Disasters by Hazardous Materials, 2005.

[16] S. Mannan, *Lees' Loss Prevention in the Process Industries*, 4th ed. Oxford, UK: Butterworth-Heinemann, 2012.

[17] CCPS, *Guidelines for Consequence Analysis of Chemical Releases*, 1st ed. Hoboken, NJ, USA: John Wiley & Sons, 1999.

[18] D. A. Crowl and J. F. Louvar, *Chemical Process Safety: Fundamentals with Applications*, 4th ed. London, UK: Pearson Education, 2019.

[19] M. Cassiani, M. B. Bertagni, M. Marro, and P. Salizzoni, "Concentration fluctuations from localized atmospheric releases," *Boundary-Layer Meteorology*, vol. 177, no. 2, pp. 461–510, 2020.

[20] F. Babich and G. Lombardi, "Statistical analysis and characterization of the indoor propagation channel," *IEEE Transactions on Communications*, vol. 48, no. 3, pp. 455–464, 2000.

[21] J. M. Smith, H. C. Van Ness, M. M. Abbott, and M. T. Swihart, *Introduction to Chemical Engineering Thermodynamics*, 8th ed. New York (NY), USA: McGraw-Hill Education, 2018.

[22] Engineering ToolBox, "Air - Density, Specific Weight and Thermal Expansion Coefficient vs. Temperature and Pressure," 2022.